Evaluation of Collection 3 MODIS LAI Products with Respect to Input Data Uncertainties – Case Study for Grasses

D. Huang, W. Yang, B. Tan, N.V. Shabanov, Y. Knyazikhin, and R. B. Myneni

Department of Geography, Boston University, Boston, MA, 02215, USA

Send correspondence to:

Dong Huang
Department of Geography
Boston University
675 Commonwealth Avenue,
Boston, MA 02215, USA
Tel.: 617-353-8846
Fax: 617-353-8399
dh@crsa.bu.edu

To be submitted for publication in
Remote Sensing of Environment
September 2003

Abstract

This paper describes the statistical nature of MODIS LAI and FPAR products arising from the relation between uncertainties in algorithm inputs and outputs, using Collection 3 MODIS LAI product from tile h10v05 containing the EOS core validation site, the Konza Prairie Biological Station. Two random variables impact the quality of retrieved LAI and FPAR fields - uncertainties in biome classification and surface reflectance measurements. It is shown that uncertainties in biome identification are primarily responsible for the disagreement between Collection 3 MODIS and measured LAI values for grasses in a 5 by 5 km area at the Konza site. Averaging over an extended area is therefore required to accumulate a sufficient number of correctly classified pixels. The performance of the main LAI-FPAR algorithm is driven by input reflectance data quality. If such data are of poor quality, the main algorithm fails with a high probability (0.7). Retrievals from the back-up algorithm in such cases will necessarily be of poor quality. For good quality input MODIS reflectance data with uncertainties typically of about 10-15%, the accuracy of LAI and FPAR retrievals from the main algorithm is about 80%. Further improvements in LAI and FPAR retrieval coverage and quality will require a better overlapping of the observational space in the red – near-infrared plane with simulated reflectances in the Look-Up-Tables of the algorithm. The analysis presented suggests that a pixel by pixel comparison between the MODIS products and fine resolution LAI and FPAR maps degraded to 1 km MODIS resolution is not valid because such an approach compares single realizations of random variables. It is essential to perform comparisons at multi-pixel-patch scale to account for uncertainties in the product arising from uncertainties in inputs to the LAI-FPAR algorithm. Research presented in this paper proceeded modifications to the MODIS LAI-FPAR algorithm implemented to generate Collection 4 product.

Nomenclature

BRF	Bi-directional Reflectance Factor
EDC DAAC	Earth resource observation system (EROS) Data Center Distributed Active Archive Center
FPAR	Fraction of Photosynthetically Active Radiation absorbed by vegetation
LAI	Leaf Area Index
LUT	Look-Up-Table
MODIS	MODerate resolution Imaging Spectroradiometer
MODAGAGG	MODIS daily AGGregated surface reflectance product
MODAPS	MODIS Adaptive Processing System
MODLAND	MODIS Land Science Team
NDVI	Normalized Difference Vegetation Index
SeaWiFS	Sea-Viewing Wide Field-of-view Sensor
SLCR	Seasonal Land Cover Regions
TM	Thematic Mapper
UMD	University of Maryland

1. Introduction

The MODerate resolution Imaging Spectroradiometer (MODIS) is an instrument on board the NASA's Terra and Aqua platforms for remote sensing of the Earth's atmosphere, oceans and the land surface (Barnes et al., 1998). The MODIS Land (MODLAND) team is responsible for the development and validation of algorithms for producing 16 geophysical data products. These include vegetation leaf area index (LAI) and fraction of photosynthetically active radiation (400-700nm) absorbed by vegetation (FPAR) (Justice et al., 2002). LAI is defined as the one sided green leaf area per unit ground area in broadleaf canopies, and as the projected needle leaf area per unit ground area in coniferous canopies. LAI and FPAR are used in models describing the exchange of fluxes of energy, mass (e.g., water and CO_2), and momentum between the surface and the planetary boundary layer (Sellers et al., 1997).

Our MODIS LAI and FPAR production activities fall under three broad categories - algorithm development, product analysis and validation. Algorithm development includes development of the at-launch algorithm (Knyazikhin et al., 1998a,b), prototyping of the algorithm (Tian et al., 2000), assessment of algorithm performance (Myneni et al., 2002; Yang et al., 2003) and algorithm refinement. Product analysis includes assessing the accuracy and quality of the product with emphasis on understanding how input data uncertainties impact the retrievals (Wang et al., 2001; this article). Validation is performed in different stages, as defined by the MODIS project, and includes comparison of the product to field measurements scaled to MODIS resolutions (Privette et al., 2002; Shabanov et al., 2003; Tian et al., 2002b,c; Wang et al., 2003a,b).

The general availability of multiple MODIS geophysical products has generated considerable interest in their validation and use in modeling studies (Privette et al., 2002; Tian et

al., 2003). The users are advised to exercise caution in view of ongoing efforts at product analysis and algorithm refinement, and also because of the largely novel nature of such products. In particular, a few validation studies have attempted to perform pixel by pixel comparisons between MODIS LAI and FPAR products with field measurements, without due attention to the statistical nature of the products and attendant details regarding the algorithm and product inter-dependencies. The aim of this effort is therefore to elucidate cogently the statistical nature of MODIS LAI and FPAR products and how this arises logically from the relation between uncertainties in algorithm inputs and outputs, using data from a simple example biome, grasses and cereal crops.

Two random variables - uncertainties in the surface reflectance product (due to correction for atmosphere and other environmental effects) and uncertainties in the biome classification product (due to misclassification and/or biome mixtures within 1 km pixel) - impact LAI and FPAR retrievals as these are two key inputs to the algorithm (uncertainties in geo-registration may be assumed negligible). Theoretical analyses indicate large uncertainties in both the land surface reflectance and biome classification products (Kaufman et. al., 1997; Lotsch et al., 2003; Vermote et. al., 1997; Vermote, 2000; Wang et al., 2001). The retrieved values of pixel LAI and FPAR should therefore be treated as observations of two random variables. The availability of validated fine resolution LAI and FPAR maps degraded to the 1 km resolution is therefore not sufficient for a pixel by pixel comparison because such an approach compares single realizations of random variables (Tian et al., 2002b,c; Wang et al., 2003a,b;). It may be essential to perform comparisons at multi-pixel-patch scale to account for uncertainties in the product.

The flow of this paper is as follow. Details relevant to the MODIS LAI and FPAR products and algorithm are discussed in section 2. Sections 3 and 4 explore the impact of uncertainties in

biome classification and surface reflectance on LAI and FPAR retrieval accuracy. The concluding remarks are presented in section 5.

2. MODIS data and the LAI -FPAR algorithm

2.1. MODIS LAI and FPAR products

The MODIS LAI and FPAR products are produced at 1 km spatial resolution daily (MOD15A1) and composited over an eight day period based on the maximum FPAR value. The eight day product (MOD15A2) is distributed to the public from the EROS Data Center Distributed Active Archive Center (EDC DAAC). The products are projected on the Integerized Sinusoidal (IS) 10-degree grid, where the globe is tiled for production and distribution purposes into 36 tiles along the east-west axis, and 18 tiles along the north-south axis, each approximately 1200 by 1200 km. The tile coordinate system starts at (0, 0) (horizontal tile number, vertical tile number) in the upper-left corner and proceeds rightwards (horizontal) and downwards (vertical). The tile in the bottom-right corner is h35v17. The product files contain four scientific data sets, output as two-dimensional HDF EOS grid fields of 1200 lines by 1200 samples. All fields are produced using the HDF uint8 data type, which is an unsigned eight bit integer variable whose values may range from 0 to 255. LAI and FPAR data sets are stored in their integer form with a scale factor (0.1 for LAI and 0.01 for FPAR) and offset (set to 0 for both LAI and FPAR) that are applied to transform the stored values to their biophysical counterparts. The quality control variables, Fpar_QC and FparExtra_QC, are integer measures without a gain or offset (Myneni et

al., 2002). Thus, for each pixel, the MODIS LAI-FPAR product consists of four numbers - LAI, FPAR, Fpar_QC and FparExtra_QC.

MODIS product versions are called Collections. Collection 1 runs from February 2000 to February 2001. Collection 3 runs from November 2000 to December 2002. Collection 4 started in January 2003 and has two streams - the forward stream processing near real time data and the reprocessing stream processing the entire archive, from February 2000 to December 2002. There was no Collection 2. Several significant modifications to the LAI-FPAR algorithm were implemented to generate the Collection 4 products. A new compositing scheme based on utilizing only the best quality retrievals has been implemented in Collection 4 replacing compositing over all retrievals in Collections 1 and 3. The AVHRR-based at-launch static LAI and FPAR biome map (Myneni et al., 1997) in Collections 1 and 3 has been replaced in Collection 4 with a MODIS data-based biome map (MOD12Q1) derived from the MODIS IGBP land cover product (Friedl et al., 2002). Ambiguities in Collections 1 and 3 quality control variables were resolved to result in a simpler and more meaningful interpretation of the flags in Collection 4.

The MODIS LAI product from tile h10v05 was selected for this investigation. This tile contains the Konza Prairie Biological Station, Manhattan, KS, USA (39.0823N, 96.56025W) which is designated as an EOS core validation site (Privette et al., 1998), selected to provide a focus for satellite, aircraft, and ground data collection of land product validation. Therefore, the analysis of biome 1 (grasses and cereal crops) MODIS Collection 3 LAI product is focused on this tile.

2.2. MODIS daily surface reflectance product

The MODIS LAI-FPAR algorithm uses an interim aggregated surface reflectance product called MODIS daily aggregated surface reflectance product (MODAGAGG) which provides daily atmospherically corrected surface reflectance at 1 km resolution in seven spectral bands centered at 648 nm (band 1), 858 nm (band 2), 470 nm (band 3), 555 nm (band 4), 1240 nm (band 5), 1640 nm (band 6), and 2130 nm (band 7). The product contains four scientific data sets - viewing and illumination angles (Angles), atmospherically corrected surface reflectance in 7 bands (Surface_Refl), quality control variables for each band (Band_QC) and aggregated 1 km observations (Aggregate_QC). The first two bits of the control variable Band_QC indicate "highest quality" (00), "intermediate quality" (01), "poor quality due to cloud effects" (10), and "poor quality due to other reason" (11). MODAGAGG is not archived and is available from the MODIS Adaptive Processing System (MODAPS) for one week after production.

2.3. Biome classification map

One important input in our approach to LAI and FPAR retrievals is the biome classification map, in which global vegetation is stratified into six canopy architectural types, or biomes. The six biomes are (1) grasses and cereal crops, (2) shrubs, (3) broadleaf crops, (4) savannas, (5) broadleaf forests and (6) needle leaf forests. These biomes span structural variations along the horizontal (homogeneous vs. heterogeneous) and vertical (single- vs. multi-storey) dimensions, canopy height, leaf type, soil brightness and climate (precipitation and temperature) space of herbaceous and woody vegetation globally. The biome map implemented in MODIS Collections 1 and 3 processing streams was a translation of the University of Maryland (UMD) 13 land

cover classes, together with the Seasonal land cover regions (SLCR) map (Lotsch et al., 2003). A new biome map based on the MODIS land cover product (MOD12) is used in Collection 4 processing (Friedl et al., 2002).

2.4. MODIS LAI-FPAR algorithm

Inputs to the operational MODIS LAI-FPAR algorithm include a global biome map (MOD12) and up to seven atmosphere-corrected surface spectral bi-directional reflectance factors (BRFs) and their uncertainties (MOD09 product). At present, only the first two of these bands (red and near-infrared) are being used because of high uncertainties in the other bands. The outputs of the algorithm are the most probable values of pixel LAI, FPAR and their respective uncertainties. A look-up-table (LUT) method is used to achieve inversion of the three-dimensional radiative transfer problem (the main algorithm). When this method fails to localize a solution, a method based on relations between the normalized difference vegetation index (NDVI) and LAI-FPAR is utilized (the back-up algorithm), together with a biome classification map, to retrieve the LAI and FPAR fields (Myneni et al., 1997). The theoretical basis of the MODIS LAI-FPAR algorithm is described in Knyazikhin et al. (1998a,b) with additional details in Panferov et al. (2001), Shabanov et al. (2000), Tian et al. (2002a) and Wang et al. (2001). The quality control variable, Fpar_QC, provides information on which of the two algorithms was used to produce the retrievals for each 1 km pixel.

The reflectance of a dense canopy in one or several directions and/or bands can be insensitive to vegetation parameters because the lower leaf-strata can be completely obscured by the upper layers. This situation results in poor quality retrievals from the so-called saturation

domain (Knyazikhin et al., 1998b). Such retrievals are flagged in the quality control variables. For each such retrieval, the lower bound of possible LAI values is evaluated. This value is to be interpreted as follows - any value above this threshold up to the maximum possible LAI can be a true solution. The arithmetic mean of the lower bound and the maximum LAI value, currently 7.0, is archived. Finally, it should be noted that the algorithm is executed irrespective of input surface reflectance quality. The users are therefore advised to use the quality control variables to select reliable retrievals.

3. Impact of uncertainties in biome classification on LAI retrievals

The assumption that a pixel uniquely contains one of six biomes impacts the retrieval of LAI and FPAR. The main algorithm either fails or produces incorrect LAI and FPAR values in case of biome misclassification or mixtures (Myneni et al., 2002; Tian et al., 2000). Therefore, the impact of biome misidentification on LAI and FPAR retrievals is assessed in this section.

The biome distribution in the tile containing the Konza site (1200 by 1200 km) is shown in Fig. 1, together with distributions in 100 by 100 km and 20 by 20 km regions centered on the Konza validation site. According to the at-launch biome map, biome 1 (grasses and cereal crops) occupies 24% of the 5 by 5 km area whereas it is 64% from ground sampling (Cohen et al., personal communication). Therefore, about 63% ($=(64\%-24\%)/64\%$) of biome 1 pixels were misclassified, mostly as broadleaf crops, and this can result in an overestimation of LAI and FPAR values - the MODIS algorithm predicts peak LAI values around six while field measurements are less than four (Fig. 2). Does this inconsistency invalidate the MODIS LAI (and FPAR) product?

As mentioned previously, two random variables impact the retrieval of LAI and FPAR fields - uncertainties in biome classification and surface reflectance measurements. The retrieved pixel LAI and FPAR values should therefore be treated as observations of random variables and, thus, averaging over an extended homogeneous area is required to reduce variations due to uncertainties. The question then arises of how big “the extended area” should be. The size of this averaging area is determined by the quality of inputs to the algorithm. This area should contain a sufficient number of pixels with reliable inputs. In the above example, 63% of biome 1 pixels with in the 5 by 5 km area were misclassified. Therefore, averages over this area cannot be used to examine variations in LAI values because the uncertainty in the biome map is too high. Figure 2, therefore, is not indicative of the quality of the MODIS LAI product.

The algorithm to cross-walk IGBP land covers to biomes, which was used to generate Collections 1 and 3 MODIS LAI and FPAR products, poorly discriminates between biomes 1 and 3 compared to the more recent biome map used in Collection 4 production (Fig. 3). The former map overestimates the frequency of biome 3 pixels in 10 by 10 km and 100 by 100 km areas centered on the Konza site. However, it correctly identifies a large homogeneous patch of biome 1 pixels present in the whole tile (Fig. 1a). The biome misidentification, therefore, has its greatest impact on LAI and FPAR retrievals in the 10 by 10 km and 100 by 100 km areas and least impact at the tile scale. This is demonstrated in Fig. 4 which shows the annual LAI profiles during two years assembled from biome 1 pixels with in the entire tile. The peak green season LAI values are around three. The LAI value derived from averaging field samples over the 5 by 5 km area at the Konza site is 3.5, but this value may or may not represent the tile-average LAI. A sampling technique that allows extrapolation of field data to a sufficiently large area is required to validate global products (Tian et al., 2002b and 2002c). Such data were not available,

and thus the tile-mean LAI can not be directly compared to field measurements. Nevertheless, it should be noted that LAI retrievals that are minimally impacted by uncertainties in biome classification are more realistic (compare Figs. 2 and 4).

The LAI profiles from 2001 and 2002 are shown in Fig. 4 by algorithm type (main and back-up, main only and back-up only). The values produced by the main algorithm vary between 1 and 3.5 during the summer months whereas the values from the back-up algorithm are much larger. The main algorithm fails if input uncertainties are high (Myneni et al., 2002; Wang et al., 2001). Pixels rejected by the main algorithm due to poor input quality are processed by the back-up algorithm that always produces a retrieval irrespective of input data quality. Thus, retrievals from the back-up algorithm are in general of poor quality. Additional investigations are required to assess the quality of back-up algorithm retrievals (Yang et al., 2003). Figure 5 shows the frequency of LAI retrievals from the main and the back-up algorithms. As most LAI values are produced by the main algorithm, the impact of LAI retrievals from the back-up algorithm is minimal in this particular example.

The analysis presented in this section suggests that uncertainties in biome identification are primarily responsible for the disagreement between MODIS and measured LAI values for grasses in a 5 by 5 km area at the Konza site. The typical overall accuracy in most biome maps is about 70-80% (Lotsch et al., 2003). This means that with a probability of about 20-30%, the biome class will be incorrectly assigned to a pixel. Averaging over an extended area is therefore required to accumulate a sufficient number of correctly classified pixels. Its size should be small enough to minimize uncertainties in the extrapolation of field data from sampling points to the entire area. On the other hand, it should be large enough to contain a sufficient number of pixels

with good input data quality needed to perform a statistical analysis. The size of the area may serve as a measure of overall uncertainty in inputs and outputs.

4. Impact of uncertainties in the MODIS surface reflectance product on LAI and FPAR retrievals

Atmosphere-corrected surface spectral bi-directional reflectance factors (BRFs) and their uncertainties are another input to the MODIS LAI-FPAR algorithm (Knyazikhin et al., 1998a). The operational MODIS surface reflectance product generation algorithm does not report actual uncertainties in the product. Only theoretical estimates, shown here in Table 1 (Vermote, 2000), generated prior to the launch of the Terra platform are available for use by the MODIS LAI-FPAR algorithm. Our prototyping of the MODIS LAI-FPAR algorithm indicates that the algorithm fails if uncertainties in the surface reflectance product exceed these values (Tian et al., 2000; Wang et al., 2001). Therefore, we first report on analysis of uncertainties in the MODIS surface reflectance product and assess their impact on LAI and FPAR retrievals later.

4.1. Uncertainties in the MODIS surface reflectance product

Variations in atmospherically corrected reflectance of a vegetated surface result from variations in canopy structure, sun-view geometry and uncertainties due to corrections for atmospheric and other environmental effects. Variations due to canopy structure and sun-view geometry are a source of information for retrieval techniques, whereas variations due to uncertainties in reflectance data are noise. These should be known to perform retrievals of highest possible quality (Wang et al., 2001).

The daily 1 km resolution atmospherically corrected surface reflectance product contains quality control variables for each spectral band indicating “highest,” “intermediate” and “poor” quality of data. We examine daily variations in the quality of surface reflectance at red (band 1) and near-infrared (band 2) channels. Tile h10v05 of the daily Collection 3 MODAGAGG data (Section 2.2) acquired from July 04 to 11th, 2001, is used in this analysis.

The temporal profile of the coefficient of variation (standard deviation divided by the mean) of MODIS surface reflectances at red and near-infrared bands is shown in Fig. 6a. Two types of coefficient were derived from the daily data. The first, using all biome 1 pixel data except for poor quality pixels. The second, using data from pixels for which the solar zenith angle differed from the mean solar zenith angle by 10%. The MODIS surface reflectance exhibits higher variation in the red band (30%-40%) compared to the near-infrared band (8%-23%). The variation due to sun angle changes is very small (<0.5%) in both of the red and the near-infrared bands (Fig. 6a). Thus, most variations in the examined MODIS surface reflectance product are due to variations in canopy structure, view angle and noise (uncertainties).

Uncertainties in reflectance data can be evaluated with data from invariant targets. Successive and repetitive reflectance measurements from these surfaces may be used to characterize the mean and variance of the data and uncertainties expressed by the coefficient of variation. If the instrument and the atmospheric correction are stable, uncertainties should be minimal because the target itself is not changing. This property is used to estimate uncertainties in the MODIS surface reflectance product.

The following terminology is used. A “valid pixel” is a pixel with Band_QC quality control variable at red and near-infrared channels set to “product produced at ideal quality” or “product produced, less than ideal quality”. Otherwise, the pixel is called “an invalid pixel”.

The biome 1 pixels in tile h10v05 are sorted into valid pixels for which at least 4 observations during the period July 4 to 11th, 2001, are available (good quality pixels). The second subset (poor quality pixels) consists of invalid pixels for which at least four observations during the same period are available. The coefficient of variation of surface reflectance, Δ_{SR}, is calculated from available observations for each pixel. This value is mainly determined by variations in view angle and noise (uncertainties) in surface reflectance product because the vegetation structure may be reasonably assumed to remain unchanged during a 4 day period.

The mean variation in good quality data is about 13% at red and 11% at near-infrared (Fig. 6b). The histograms for poor quality data are wider, especially for the red band (Fig. 6c). The mean coefficient of variation for the near-infrared band is about 30%. The histogram corresponding to the red band has two peaks at 13% and 70%. This result suggests that, with a high probability, the MODAGAGG quality control variables provide correct information about the quality of atmospherically corrected surface reflectance. This can be further ascertained by removing the effects of variations in view angle.

The histogram of view angles under which poor quality pixels were observed is wide (Fig. 7a). To estimate the impact of this variation on surface reflectance, coefficients of variation of view angle, Δ_{view}, and surface reflectance, Δ_{SR}, were calculated for each poor quality pixel using four MODIS observations. The histograms of Δ_{SR} and Δ_{view} are shown in Fig. 6c and Fig. 7b. These were then used to derive the regression curve $\delta_{SR} = E(\Delta_{SR}, \Delta_{view} = \delta_{view})$ of Δ_{SR} with respect to variation in the view angle. Here $E(\Delta_{SR}, \Delta_{view} = \delta_{view})$ is the expectation of Δ_{SR} for the condition Δ_{view} takes the value δ_{view}. The regression curve δ_{SR} is the best possible prediction of Δ_{SR} given a realized value of Δ_{view} (Bronshtein and Semendyayev, 1985). The regression curve and its linear approximation $\delta_{SR} = 0.3\delta_{view} + 46\%$ is shown in Fig. 7c. Variation in poor quality

reflectances is about 46% when view angle variations are insignificant (δ_{view} <8%) – this can be taken as an estimate of the uncertainty due to correction for atmospheric and other environmental effects. Thus, we conclude that the MODAGAGG quality control variables provide correct information about the quality of atmospherically corrected MODIS surface reflectance data. Similar analysis suggests that uncertainties in good quality data are about 10-15%.

From the foregoing analysis, we infer that the average uncertainties in the MODIS surface reflectance product are about 10-15% for good quality data (data from pixels with MODAGAGG Band_QC quality control variable at red and near-infrared channels set to "product produced at ideal quality" or "product produced, less than ideal quality") and about 45% for poor quality data (data from pixels with other values of MODAGAGG Band_QC).

4.2. Impact of surface reflectance uncertainties on LAI-FPAR retrievals

The ratio of pixels with valid data, as defined in section 4.1, to the total number of grasses and cereal crops (biome 1) pixels in the tile h10v05 is shown in Fig. 8a. About 38% of the pixels contain valid data, useful as inputs to the LAI-FPAR algorithm. This number changes by date and may be as low as 10%. This variation may be due to clouds, atmospheric conditions and other environmental factors not accounted in the surface reflectance retrieval algorithm. The main LAI-FPAR algorithm is expected to fail if uncertainties in the surface reflectance product exceed theoretical estimates shown in Table 1, in which case the back-up algorithm is triggered to estimate LAI and FPAR. The quality control variable Fpar_QC provides information about this algorithm path. A question then arises whether or not this is the case operationally.

The MODIS LAI-FPAR algorithm was executed using the Collection 3 MODAGAGG surface reflectance product for the tile h10v05. The distribution of valid and invalid pixels processed by the main and back-up algorithms is shown in Fig. 8b. According to the quality control variable "Band_QC", 62% of the surface reflectance product acquired during July 4 to 11th, 2001 (Fig. 8a), should be treated as unreliable input to the LAI-FPAR algorithm (Fig. 8a). About 72% of the invalid pixels were processed by the back-up algorithm, i.e., the main algorithm fails with a probability of about 72% (Fig. 8b, $47\%/(47\%+18\%)=72\%$), if surface reflectance quality is low. However, the main algorithm processed only 40% of the pixels with valid data (Fig. 8b, $14\%/(14\%+21\%)=40\%$). This may be an indication of deficiencies in LAI-FPAR algorithm physics or in the definition of valid data based on input quality indicators (Section 4.1). When the algorithm flow is examined on a daily basis, it appears that poor input data quality is the dominant factor for failure of the main algorithm (Fig. 8c). The fraction of valid pixels for which the main algorithm produces a retrieval, defined here as the retrieval index, exhibits unpredictable behavior (Fig. 8d). Mean retrieval indices for valid and invalid data are 0.4 and 0.28, respectively, i.e., valid data are more likely to result in successful retrievals by the main algorithm, as expected. However, the strange day to day variation of the main algorithm retrieval index requires a detailed investigation of the MODIS surface reflectance product and the associated algorithm, which is beyond the scope of this article.

Thus, the main radiative transfer based LAI-FPAR algorithm fails to produce a retrieval, with a probability of 72%, if the input reflectance data are invalid (as defined in section 4.1), as flagged by MODAGAGG quality indicators. However for 28% of similarly defined invalid pixels, the main algorithm produces a retrieval. What is the quality of such retrievals? Further,

only about 40% of the valid pixels are processed by the main algorithm. What about the other 60%?

The average uncertainty of reflectance data in good quality pixels is about 10-15% (good quality pixels are valid pixels with at least 4 days of data during the period July 4 to 11th, 2001; see Section 4.1). The uncertainty threshold in the operational LAI and FPAR algorithm is 12.5% (Wang et al., 2001). Therefore, some pixels with good quality data for which the main algorithm fails may actually have uncertainties greater than the acceptable level of 12.5%. As shown in Figs. 6b and 6c, both good quality and poor quality pixels include, with a certain probability, observations with both low and high uncertainties (poor quality pixels are invalid pixels with at least 4 days of data during the period July 4 to 11th, 2001; see Section 4.1). The question is, if good quality data with high uncertainties are removed, does this increase the success rate of the main algorithm? Similarly, does the main algorithm success rate increase for poor quality pixels with low uncertainties? If this is the case, then, the main algorithm retrievals may indeed be treated as of maximum possible quality given the uncertainty threshold (Wang et al., 2001).

The pixels with good and poor quality data were further sorted in to subsets with uncertainties greater or lesser than 13% in order to perform a more accurate analysis of the impact of uncertainties on LAI retrievals. The four pixel groups are abbreviated as GL, GH, PL, and PH. The first letter indicates whether good (G) or poor (P) quality pixels were used to form a subset. The second letter signifies the uncertainty level, namely, low δ_{SR}<13% (L), or high δ_{SR}>13% (H). The subsets GL and PL are sufficiently well localized in the red – near-infrared reflectance space (Fig. 9) and occupy the space bounded by $0.02 \le \text{red} \le 0.2$ and $0.1 \le \text{near-infrared} \le 0.6$. There is overlap between GL and GH groups of pixels. The upper boundary of the subset PH forms a line for which near-infrared reflectance is equal to red reflectance. The

Normalized Difference Vegetation Index (NDVI) for these boundary pixels is close to 0 (clouds or bare surfaces).

The retrieval index, defined as the fraction of pixels for which the main algorithm produced a retrieval, was 65%, 44%, 64% and 22% for the subsets GL, GH, PL, and PH, respectively. Therefore, the main algorithm success rate is about 64% if the input surface reflectance data have low uncertainties, irrespective of the MODAGAGG quality indicators. This reinforces our previous result that, with a high probability, main algorithm failures are related to input data uncertainties. The success rate of the main algorithm for GH pixels is 44% which may be explained by the fact that uncertainties in this subset are distributed between 13 and 20% with a maximum at 13% - that is, these pixels are on the verge of acceptable accuracy (Fig. 6b).

A more refined analysis was performed by splitting the good and poor quality pixels in to narrow classes with respect to δ_{SR}. The retrieval index as a function of uncertainties δ_{SR} in input surface reflectances is shown in Fig. 10a. The retrieval index is a decreasing function of input data uncertainties, as expected. A sufficiently high global coverage can be achieved if $\delta_{SR} \leq 15\%$.

The retrieval indices do not indicate retrieval quality, rather the spatial coverage of retrieved fields. Therefore, we performed the following analysis to estimate the impact of input uncertainties on LAI retrieval quality (Fig. 10b). The coefficient, δ_{LAI}, of variation of retrieved LAI was calculated for each pixel, separately from the subsets of good and poor quality pixels, and taken as a measure of uncertainties in LAI retrievals. The variation in LAI values due to uncertainties in reflectances of good and poor quality pixels is about 10% and 30%, respectively. The poor quality pixel histogram is wide, indicating low retrieval quality (Fig. 10b).

The pixels were further split into narrow classes with respect to δ_{SR}. For each pixel, the coefficient of variation, Δ_{LAI}, of LAI was calculated. A regression curve $\delta_{LAI} = E(\Delta_{LAI}, \Delta_{SR} = \delta_{SR})$

of Δ_{LAI} with respect to variation in surface reflectance at red was derived using the fields Δ_{LAI} and Δ_{SR}. This regression curve, characterizing uncertainties in LAI retrievals as a function of uncertainties in MODIS surface reflectance at the red spectral band is shown in Fig. 10c. Uncertainties in retrieved LAI values exceed uncertainties in surface reflectance below a threshold value of 20% indicating that the upper limit of Collection 3 LAI and FPAR product accuracy is 80%. Above this threshold value, LAI and FPAR uncertainties are linearly related to surface reflectance uncertainties, suggesting that reductions in LAI and FPAR accuracy below 80% are driven by inaccuracies or uncertainties in the surface reflectance product.

From the foregoing analysis, we infer that the performance of the main LAI-FPAR algorithm is driven by input reflectance data quality. If such data are of poor quality, the main algorithm fails with a high probability. Retrievals from the back-up algorithm in such cases will necessarily be of poor quality. For good quality input data with uncertainties typically of about 10-15%, the accuracy of LAI and FPAR retrievals from the main algorithm is about 80%, which argues for further improvements in algorithm physics, and this is discussed below.

4.3. Discrepancy between observed and simulated MODIS vegetation reflectances

The results presented in section 4.2 indicate that the retrieval index for data with uncertainties below 15% is between 65% and 70% (Fig. 10a). There appears to be a threshold limit to input reflectance uncertainties (15-20%) below which retrieval uncertainties do not necessarily decrease with increasingly accurate input reflectance data (Fig. 10c). Therefore, exploitation of any further increases in overall MODIS reflectance data quality will require improvements to the MODIS LAI-FPAR algorithm physics.

First, let us first examine the general magnitudes of spectral surface reflectance from MODIS. The average reflectance of biome 1 evaluated from eight consecutively dated Collection 3 MODAGAGG data in tile h10v05 is 0.09 at red and 0.35 at near-infrared spectral bands (Table 2). The MODIS red reflectance is comparable to that from the Sea-Viewing Wide Field-of-view Sensor (SeaWiFS) and the Landsat Thematic Mapper (TM) (Wang et al., 2001 and Tian et al., 2000). However, the MODIS near-infrared reflectance is substantially higher than SeaWiFS and Landsat TM data. Although one may expect some difference in reflectance values between the various sensors, due to differences in sensor characteristics, spatial resolution and area of averaging, the MODIS values should be in between Landsat TM and SeaWiFS values as the reflectance of a vegetated surface at near-infrared increases with spatial resolution (Tian et al., 2000).

The above anomaly points to a mismatch between the simulated and observed surface reflectance patterns that presently limits retrieval quality. For instance, compare the distribution of biome 1 pixels in the red - near-infrared reflectance space as presently implemented in Collection 3 LAI and FPAR algorithm (Fig. 11a) with subsets GL and PL (Section 4.2 and shown in Fig. 9). It is clear that the main algorithm cannot reproduce the whole set of observations. The following analysis quantifies the disagreement between simulated and observed MODIS reflectances.

Let GL, GH, PL, and PH denote the sets as defined in section 4.2 (Fig. 9) and C3 be the set of simulated surface reflectances stored in the Look-Up-Tables of Collection 3 MODIS LAI-FPAR main algorithm (Fig. 11a). Introduce an indicator function γ(RED, NIR) for each set on the red – near-infrared plane whose value is 1 if there is a point of the given set at location (RED, NIR), and zero otherwise. In other words, the indicator function for a given set takes on the value

1 at “black dots” in Fig. 9 and zero otherwise. These functions can be used to calculate areas on the red – near-infrared plane occupied by these sets as well as sets obtained by intersection ($\bigcap$) and union ($\bigcup$) between them. Let A and B represent one of the set mentioned above, and γ_A and γ_B be the corresponding indicator functions. We define areas of A, B, $A \bigcap B$ and $A \bigcup B$ as follows:

$$A = \sum \gamma_A(\text{Red}, \text{NIR}), \quad (1)$$

$$A \bigcap B = \sum \gamma_A(\text{RED}, \text{NIR}) \gamma_B(\text{RED}, \text{NIR}), \quad (2)$$

$$A \bigcup B = \sum \gamma_A(\text{RED}, \text{NIR}) \gamma_B(\text{RED}, \text{NIR}) + |\gamma_A(\text{RED}, \text{NIR}) - \gamma_B(\text{RED}, \text{NIR})|. \quad (3)$$

The areas of sets GL, GH, PL, PH and C3 as well as areas of their intersections and unions are given in Table 3. This table also includes Collection 4 simulated surface reflectances, denoted as C4 - note that C4 is the first reprocessing of the entire MODIS archive as mentioned in section 2.1.

The sets GL and PL were identified as containing reliable surface reflectances, that is, with uncertainties less than the threshold in Collection 3 MODIS LAI and FPAR algorithm (12.5%). The areas of GL, PL, GL $\bigcap$ PL and GL $\bigcup$ PL are 2214, 762, 704 and 2274, respectively. The area occupied by pixels from the PL which is not in the GL is PL–(GL $\bigcap$ PL)=58. Thus, only 100%×58/GL=2.6% of the pixels from GL are outside of the set PL, i.e., PL is a subset of GL. In other words, the reflectance of pixels flagged by the MODAGAGG Band_QC as unreliable, but identified by our analysis as reliable, occupy the same space in the red – near-infrared plane as those flagged by the MODAGAGG Band_QC as reliable. The probability of GL $\bigcap$ PL/GL $\bigcup$ PL, i.e., part of acceptable quality reflectance flagged as unreliable, is 0.32. These results explain the high retrieval indices for the sets GL and PL (Section 4.2).

To compare the set of reliable observations with the set of simulated reflectances stored in the Look-Up-Tables of Collection 3 MODIS LAI-FPAR main algorithm, note that C3=2216, C3$\cap$GL=755, and C3$\cup$GL=3585. The simulated data occupy about 100%×C3$\cap$GL/GL=34% of the area formed by observations. The probability that an observed reflectance falls in the region of simulated reflectances is 65%, as inferred from the retrieval index for the set GL. The area GL−C3$\cap$GL consists of pixels for which the main algorithm fails. The histograms of red and near-infrared reflectance of pixels from C3$\cap$GL and GL−C3$\cap$GL are shown in Figs. 11b and 11c. The main algorithm mostly fails for pixels with nearly-constant red and near-infrared reflectances, 0.03 and 0.35, respectively. However, such pixels also have low values of coefficient of variation of surface reflectance, $\delta_{SR,}$ and thus, these pixels are attributed to GL. The corresponding NDVI value is 0.84, which is not representative of biome 1 canopies at 1 km spatial resolution. Thus, we conclude that the mismatch between the observed MODIS and simulated Collection 3 surface reflectances is due both to deficiencies in physics of the LAI and FPAR and atmospheric correction algorithms. Further improvements in LAI and FPAR retrieval coverage and quality will require a better overlapping of the observational space in the red – near-infrared plane by simulated reflectances in the Look-Up-Tables of the algorithm.

5. Concluding remarks

The aim of this effort was to elucidate the statistical nature of MODIS LAI and FPAR products and how this arises logically from the relation between uncertainties in algorithm inputs and outputs, using data from a simple example biome, grasses and cereal crops. The Collection 3 MODIS LAI product from tile h10v05 containing the EOS core validation site, the

Konza Prairie Biological Station, was selected for this investigation. Two random variables impact the quality of retrieved LAI and FPAR fields - uncertainties in biome classification and surface reflectance measurements.

The analysis suggests that uncertainties in biome identification are primarily responsible for the disagreement between Collection 3 MODIS and measured LAI values for grasses in a 5 by 5 km area at the Konza site. Averaging over an extended area is therefore required to accumulate a sufficient number of correctly classified pixels. Its size should be small enough to minimize uncertainties in the extrapolation of field data from sampling points to the entire area. On the other hand, it should be large enough to contain a sufficient number of pixels with good input data quality needed to perform a statistical analysis. The size of the area may serve as a measure of overall uncertainty in inputs and outputs of the LAI-FPAR algorithm.

The analysis indicates that the average uncertainties in the MODIS surface reflectance product are about 10-15% for good quality data (data from pixels with MODAGAGG Band_QC quality control variable at red and near-infrared channels set to “product produced at ideal quality” or “product produced, less than ideal quality”) and about 45% for poor quality data (data from pixels with other values of MODAGAGG Band_QC).

The performance of the main LAI-FPAR algorithm is driven by input reflectance data quality. If such data are of poor quality, the main algorithm fails with a high probability (0.7). Retrievals from the back-up algorithm in such cases will necessarily be of poor quality. For good quality input data with uncertainties typically of about 10-15%, the accuracy of LAI and FPAR retrievals from the main algorithm is about 80%. Further improvements in LAI and FPAR retrieval coverage and quality will require a better overlapping of the observational space in the red – near-infrared plane by simulated reflectances in the Look-Up-Tables of the algorithm.

Finally, the analysis presented suggests that a pixel by pixel comparison between the MODIS products and fine resolution LAI and FPAR maps degraded to 1 km MODIS resolution is not valid because such an approach compares single realizations of random variables. It is essential to perform comparisons at multi-pixel-patch scale to account for uncertainties in the product arising from uncertainties in inputs to the LAI-FPAR algorithm.

Acknowledgments

This work was funded by the NASA Earth Science Enterprise under the MODIS contract to Boston University. The authors thank Drs. Vermote, El Saleous, Roy, Wolfe and Justice for their respective contributions to MODIS which made this work possible. This analysis was motivated in part by certain preliminary results reported by the BigFoot team at a MODIS workshop.

References

Barnes, W.L., Pagano, T.S., & Salomonson, V.V. (1998). Prelaunch characteristics of the Moderate Resolution Imaging Spectroradiometer (MODIS) on EOS-AM1. *IEEE Transactions on Geoscience and Remote Sensing, 36*, 1088-1100.

Bronshtein, I.N., & Semendyayev, K.A. (1985). *Handbook of Mathematics*, Springer, Berlin, pp. 973.

Friedl, M.A., McIver, D.K., Hodges, J.C.F., Zhang, X.Y., Muchoney, D., Strahler, A.H., Woodcock, C.E., Gopal, S., Schneider, A., & Cooper, A. (2002). Global land cover mapping from MODIS: Algorithms and early results. *Remote Sensing of Environment*, 183, 287-302.

Justice, C.O., Townshend, J.R.G., Vermote, E.F., Masuoka, E., Wolfe R.E., Saleous N., Roy D.P., & Morisette J. T. (2002). An overview of MODIS land data processing and product status. *Remote Sensing Of Environment*, 83, 3-15.

Kaufman, Y.J., Tanre, D., Remer, L., Vermote, E.F., Chu, A., & Holben, B.N. (1997). Operational remote sensing of tropospheric aerosol over the land from EOS-MODIS. *Journal of Geophysical Research*, 102(14), 170351-17068.

Knyazikhin, Y., Martonchik, J.V., Diner, D.J., Myneni, R.B., Verstraete, M., Pinty, B., & Gorbon, N. (1998b). Estimation of vegetation canopy leaf area index and fraction of absorbed photosynthetically active radiation from atmosphere-corrected MISR data. *Journal of Geophysical Research*, 103, 32239-32256.

Knyazikhin, Y., Martonchik, J.V., Myneni, R.B., Diner, D.J., & Runing, S.W. (1998a). Synergistic algorithm for estimating vegetation canopy leaf area index and fraction of absorbed photosynthetically active radiation from MODIS and MISR data. *Journal of Geophysical Research*, 103, 32257-32275.

Lotsch, A., Tian, Y., Fridel, M.A., & Myneni, R.B. (2003). Land cover mapping in support of LAI and FAPAR retrievals from EOS-MODIS and MISR: Classification methods and sensitivities to errors. *International Journal of Remote Sensing*, 24, 1997-2016.

Myneni, R.B., Nemani, R.R. & Running S.W. (1997). Estimation of global leaf area index and absorbed par using radiative transfer models. *IEEE Transactions on Geosciences and Remote Sensing*, 35, 1380-1393

Myneni, R.B., Hoffman, S., Knyazikhin, Y., Privette, J.L., Glassy, J., Tian, Y., Wang, Y., Song, X., Zhang, Y., Smith, G.R., Lotsch, A., Friedl, M., Morisette, J.T., Votava, P., Nemani, R.R., & Running, S.W. (2002). Global products of vegetation leaf area and fraction absorbed PAR from year one of MODIS data. *Remote Sensing of Environment*, 83, 214-231.

Panferov, O., Knyazikhin, Y., Myneni, R.B., Szarzynski, J., Engwald, S., Schnitzler, K.G., & Gravenhorst, G. (2001). The role of canopy structure in the spectral variation of transmission and absorption of solar radiation in vegetation canopies. *IEEE Transactions on Geosciences and Remote Sensing*, 39, 241-253.

Privette, J.L., Myneni, R.B., Morisette, J.T., & Justice, C.O. (1998). Global validation of EOS LAI and FPAR products. *The Earth Observer*, 10, 39-42.

Privette, J. L., Myneni, R. B., Knyazikhin, Y., Mukufute, M., Roberts, G., Tian, Y., Wang, Y., & Leblanc, S.G. (2002). Early spatial and temporal validation of MODIS LAI product in Africa. *Remote Sensing of Environment*, 83, 232-243.

Sellers, P.J., Randall D.A., Betts A.K., Hall F.G., Berry J.A., Collatz G.J., Denning, A.S., Mooney H.A., Nobre C.A., Sato N., Field C.B., & Henderson-sellers A. (1997). Modeling the exchanges of energy, water, and carbon between continents and the atmosphere. *Science*, 275:502-509.

Shabanov, N.V., Knyazikhin, Y., Baret, F., & Myneni, R.B. (2000). Stochastic modeling of radiation regime in discontinuous vegetation canopy. *Remote Sensing of Environment*, 74,125-144.

Shabanov, N.V., Wang, Y., Buermann, W., Dong, J., Hoffman, S., Smith, G.R., Tian, Y., Knyazikhin, Y., & Myneni, R.B. (2003). Effect of foliage spatial heterogeneity in the MODIS LAI and FPAR algorithm over broadleaf forests. *Remote Sensing of Environment*, 85, 410-423.

Tian, Y., R.E. Dickinson, Zhou, L., Zeng, X., Dai, Y., Myneni, R.B., Knyazikhin, Y., Zhang, X., Friedl, M., Yu, H., Wu, W., & Shaikh, M. (2003). Comparison of seasonal and spatial variations

of LAI/FPAR from MODIS and Common Land Model. *Journal of Geophysical Research*, (in press).

Tian, Y., Wang, Y., Zhang, Y., Knyazikhin, Y., Bogaert, J., & Myneni, R.B. (2002a). Radiative transfer based scaling of LAI/FPAR retrievals from reflectance data of different resolutions. *Remote Sensing of Environment*, 84, 143-159.

Tian, Y., Woodcock, C.E., Wang, Y., Privette, J.L., Shabanov, N.V., Zhou, L., Zhang, Y., Buermann, W., Dong, J., Veikkanen, B., Hame, T., Anderson, K., Ozdogan, M., Knyazikhin, Y., & Myneni, R.B. (2002b). Multiscale analysis and validation of the MODIS LAI Product. I. Uncertainty assessment. *Remote Sensing of Environment*, 83, 414 430.

Tian, Y., Woodcock, C.E., Wang, Y., Privette, J.L., Shabanov, N.V., Zhou, L., Zhang, Y., Buermann, W., Dong, J., Veikkanen, B., Hame, T., Anderson, K., Ozdogan, M., Knyazikhin, Y., & Myneni, R.B. (2002c). Multiscale analysis and validation of the MODIS LAI Product. II. Sampling strategy. *Remote Sensing of Environment*, 83, 431-441.

Tian, Y., Zhang, Y., Knyazikhin, Y., Myneni, R.B., Glassy, J., Dedieu, G., & Running, S.W. (2000). Prototyping of MODIS LAI and FPAR algorithm with LASUR and LANDSAT data. *IEEE Transactions on Geoscience and Remote Sensing*, 38, 2387-2401.

Vermote, E. (2000). Product accuracy/Uncertainty: MOD09, surface reflectance; atmospheric correction algorithm product. In *MODIS Data Products Catalog* (EOS AM Platform), http://modarch.gsfc.nasa.gov/MODIS/RESULTS/DATAPROD/.

Vermote, E.F., El Saleous, N.Z., Justice, C.O., Kaufman, Y.J., Privette, J., Remer, L., Roger, J. C., & Tanre, D. (1997). Atmospheric correction of visible to middle infrared EOS-MODIS data over land surface, background, operational algorithm and validation. *Journal of Geophysical* Research, 102(14), 17131-17141.

Wang, Y., Buermann, W., Stenberg, P., Smolander, H., Hame, T., Tian, Y., Hu, J., Knyazikhin, Y.., & Myneni, R.B. (2003a). A new parameterization of canopy spectral response to incident solar radiation: Case study with hyperspectral data from pine dominant forest. *Remote Sensing of Environ*ment, 85, 304-315.

Wang, Y., Tian, Y., Zhang, Y., El-Saleous, N., Knyazikhin, Y., Vermote, E., & Myneni, R.B. (2001). Investigation of product accuracy as a function of input and model uncertainities: Case study with SeaWiFS and MODIS LAI/FPAR Algorithm. *Remote Sensing of Environment*, 78, 296-311.

Wang, Y., Woodcock, C.E., Buermann, W., Stenberg, P., Voipio, P., Smolander, H., Hame, T., Tian, Y., Hu, J., Knyazikhin, Y., & Myneni, R.B. (2003b). Validation of the MODIS LAI product in coniferous forest of Ruokolahti, Finland. *Remote Sensing of Environment*, (in review).

Yang, W., Stroeve, J.C., Huang, D., Shabanov, N.V., Knyazikhin, Y., & Myneni, R.B. (2003). Analysis of the MODIS LAI and FPAR collections 1 and 3 data set time series from July 2000 to December 2002. *Remote Sensing of Environment*, (in press).

FIGURE CAPTIONS

Fig. 1. Spatial distribution of biomes in the entire tile (panel a) and in 100 by 100 km (panel b) and 20 by 20 km (panel c) areas around the Konza validation site, as contained in the at-launch biome map. A 5 by 5 km area where field measurements were performed is shown in Panel (c). The at-launch biome map identifies biome 3 (Broadleaf Crops) as the most probable biome type within the 5 by 5 km area while filed measurements show that only 0.3% of this area are occupied by Broadleaf Crops.

Fig. 2. Seasonal variation in mean LAI averaged over a 5 by 5 km area near the Konza Prairie Biological Station centered at (39.0823N, 96.56025W). LAI values produced by the main algorithm were used. Retrievals for 2001 are shown in panel (a) and 2002 in panel (b). The MODIS algorithm overestimates LAI and FPAR values compared to field measurements.

Fig. 3. Distribution of biomes with in 10 by 10 km and 100 by 100 km areas centered on the Konza site and in the entire tile derived from the at-launch biome map (Panels a, c and e) and the more recent MODIS data based biome map (Panels b, d, and f).

Fig. 4. Annual course of LAI during 2001 and 2002 for biome 1 pixels (grasses and cereal crops) in the Konza tile h10v05. Panels (a) and (b) show retrievals from both algorithms, while panels (c) and (d) show retrievals from the main algorithm and panels (e) and (f) depict retrievals from the back-up algorithm.

Fig. 5. Percentage of biome 1 pixels in the tile h10v05 processed by the main and the NDVI-based back-up algorithm.

Fig. 6. Variations in MODIS surface reflectance data. (a) Daily variations in MODIS surface reflectances at red (RED) and near-infrared (NIR) spectral bands. Legends "RED, regardless of solar angle" and "NIR, regardless of solar angle" correspond to coefficients of variation (standard deviation/mean) calculated using all biome 1 (grasses and cereal crops) pixels in tile h10v05. Coefficients of variation calculated from pixels for which differences in the solar zenith angle did not exceed 10% are labeled as "Red, for Δ_{SZA}<10%" and "NIR, for Δ_{SZA}<10%". (b) Histogram of the coefficients of variation of MODIS surface reflectance at red and near-infrared bands derived for "Good Quality" data. (c) Same as (b) except that the coefficients of variation were derived from "Poor Quality" data. See section 4.1 for definitions of such data.

Fig. 7. Variations in MODIS surface reflectance data due to view angle changes. (a) Histogram of view angles for the set of "Poor Quality" pixels. (b) Histogram of δ_{view} (coefficient of variation of view angle) for the set of "Poor Quality" pixels. (c) Best possible prediction of variation, δ_{SR}, in surface reflectance at Red given variation, δ_{view}, in the view angle. The linear approximation of the regression curve is shown as straight line, $\delta_{SR} = 0.3\delta_{view} + 46\%$.

Fig. 8. Algorithm flow as function of input surface reflectance quality. (a) The ratio of valid pixels to total biome 1 (grasses and cereal crops) pixels, in percentage. The average ratio is shown here as a dashed line. (b) Distribution of valid and invalid pixels processed by the main

and back-up algorithms. (c) Daily distribution of valid and invalid pixels processed by the main and back-up algorithms. (d) Daily variation in the retrieval index for valid and invalid pixels. The retrieval index is the fraction of processed pixels for which the main algorithm produces a retrieval. Average indices are shown in this plot as a dashed line.

Fig. 9. Distribution in the red and near-infrared reflectance space of MODIS surface reflectance data from pixels with (a) good quality data and uncertainties less than 13% (GL) (b) good quality data and uncertainties greater than 13% (GH), (c) poor quality data and uncertainties less than 13% (PL) and (d) poor quality data and uncertainties greater than 13% (PH).

Fig 10. Impact on input reflectance data uncertainties on retrieval index and retrieval quality. (a) Retrieval index as a function of uncertainties in input surface reflectances. (b) Histograms of the coefficient of variation of LAI, δ_{LAI}, derived from good and poor quality pixels. (c) Uncertainties in LAI retrieval as a function of uncertainties in input surface reflectances.

Fig. 11. Comparison of simulated and observed MODIS surface reflectances. (a) Distribution of biome 1 pixels in the red and near-infrared reflectance space as presently implemented in the Collection 3 MODIS LAI and FPAR algorithm. (b) Histogram of surface reflectance in the red, NIR bands and NDVI of pixels for which the main algorithm produces a LAI value. (c) Same as (b) except that for these pixels the main algorithm fails.

TABLE CAPTIONS

Table 1. Theoretical estimates made prior to launch of Terra MODIS relative uncertainties in atmospherically corrected surface reflectances (Vermote, 2000).

Table 2. Spectral reflectance magnitudes of biome 1 (grasses and cereal crops) from MODIS, SeaWiFS and Landsat TM data.

Table 3. Comparison of observed and simulated surface reflectances.

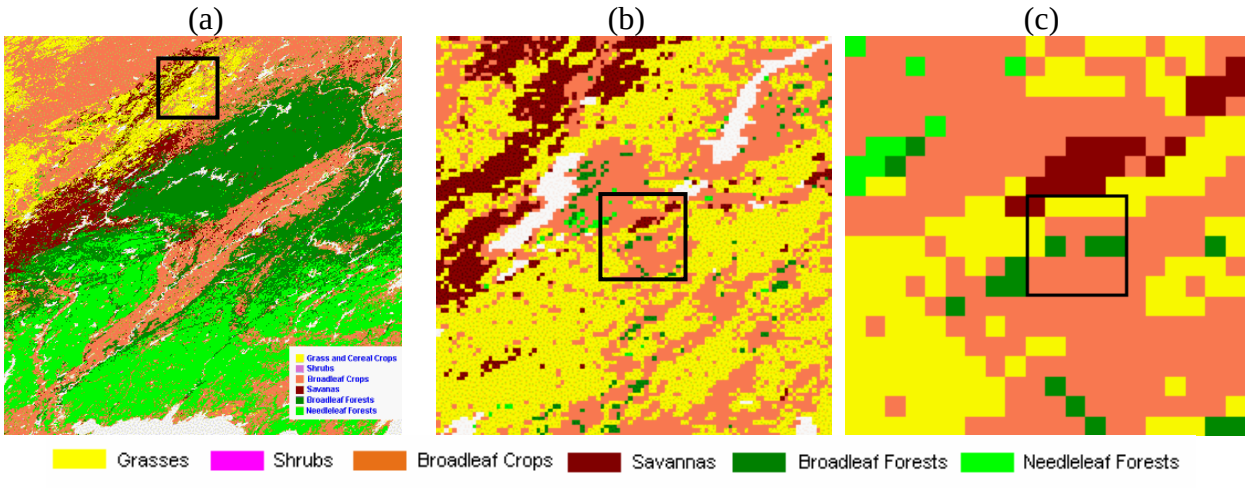

Fig. 1. Spatial distribution of biomes in the entire tile (panel a) and in 100 by 100 km (panel b) and 20 by 20 km (panel c) areas around the Konza validation site, as contained in the at-launch biome map. A 5 by 5 km area where field measurements were performed is shown in Panel (c). The at-launch biome map identifies biome 3 (Broadleaf Crops) as the most probable biome type within the 5 by 5 km area while filed measurements show that only 0.3% of this area are occupied by Broadleaf Crops.

(a) (b)

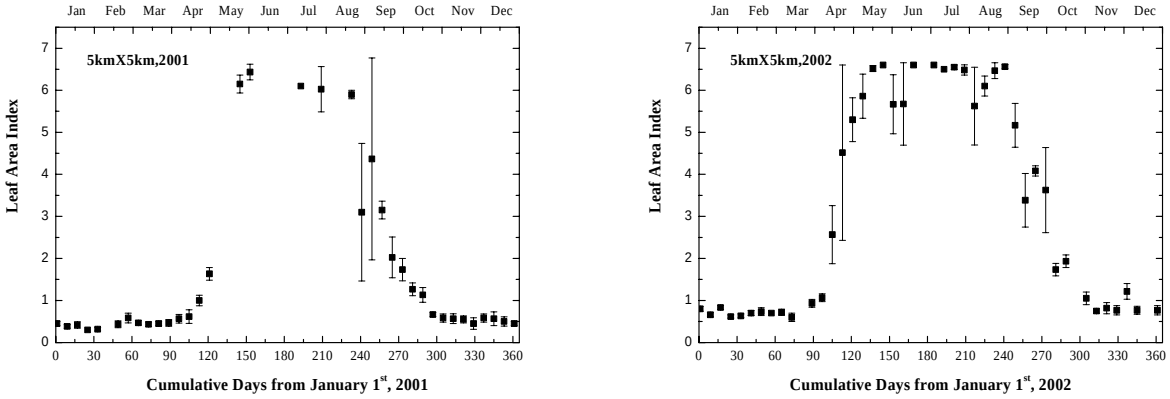

Fig. 2. Seasonal variation in mean LAI averaged over a 5 by 5 km area near the Konza Prairie Biological Station centered at (39.0823N, 96.56025W). LAI values produced by the main algorithm were used. Retrievals for 2001 are shown in panel (a) and 2002 in panel (b). The MODIS algorithm overestimates LAI and FPAR values compared to field measurements.

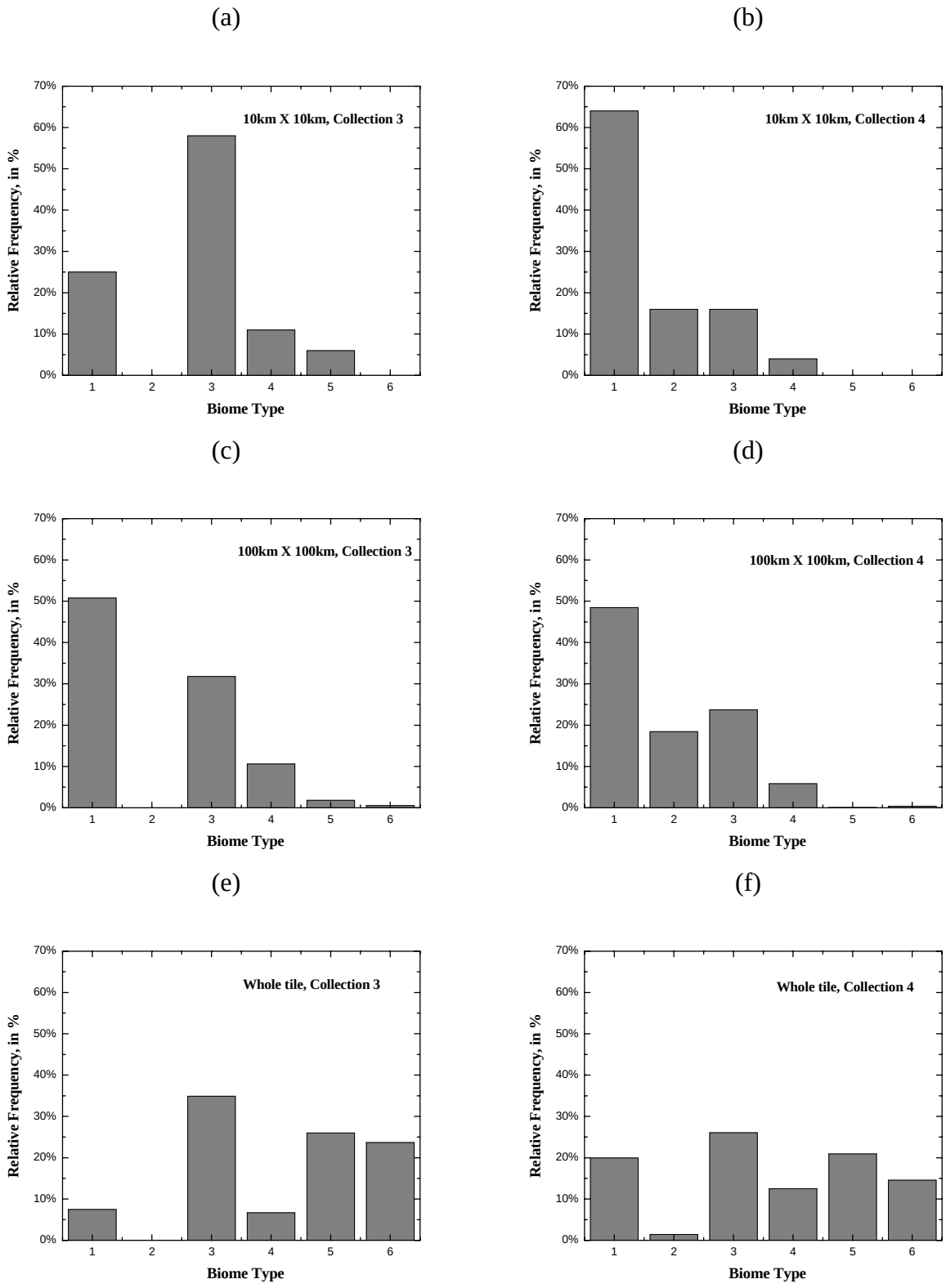

Fig. 3. Distribution of biomes with in 10 by 10 km and 100 by 100 km areas centered on the Konza site and in the entire tile derived from the at-launch biome map (Panels a, c and e) and the more recent MODIS data based biome map (Panels b, d, and f).

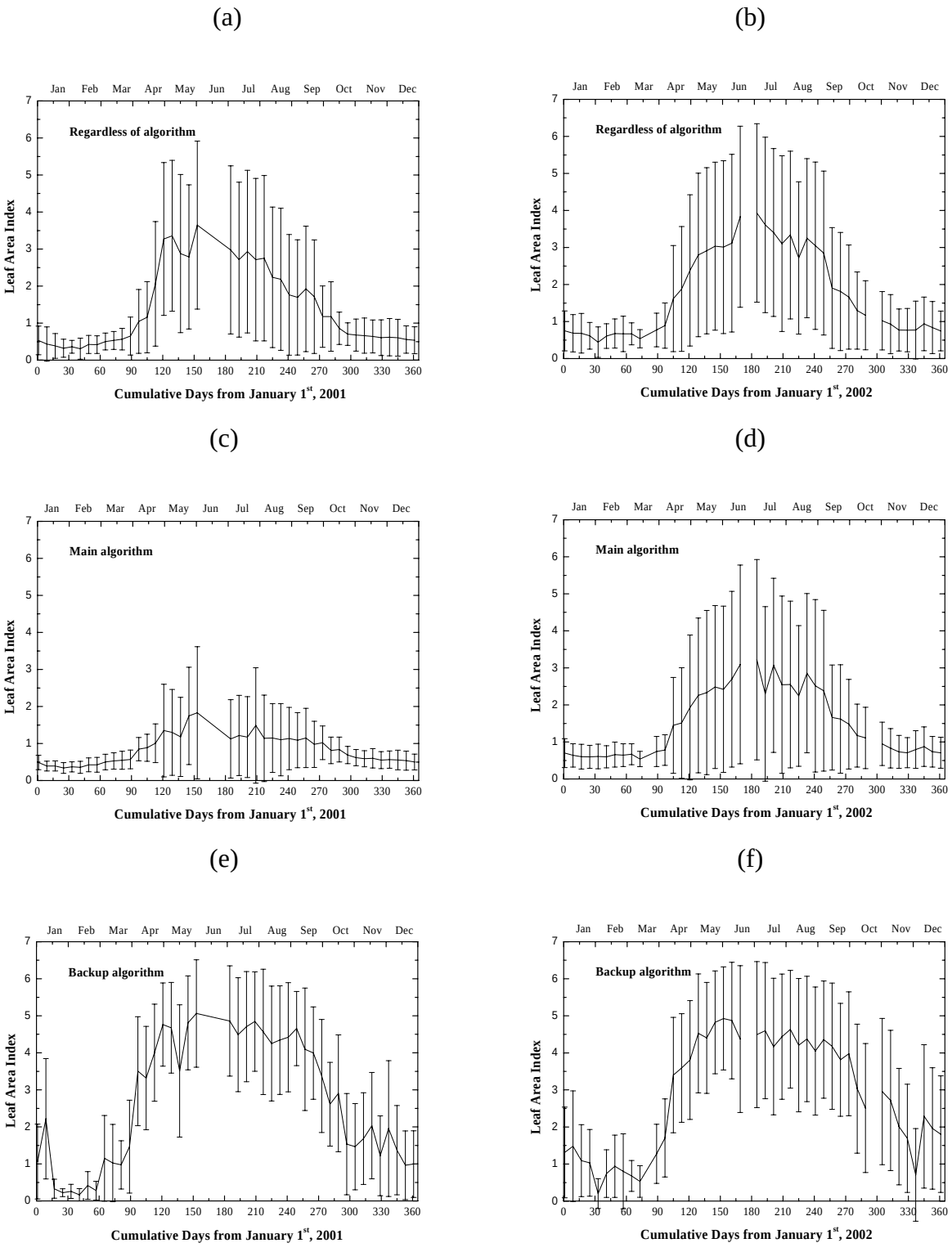

Fig. 4. Annual course of LAI during 2001 and 2002 for biome 1 pixels (grasses and cereal crops) in the Konza tile h10v05. Panels (a) and (b) show retrievals from both algorithms, while panels (c) and (d) show retrievals from the main algorithm and panels (e) and (f) depict retrievals from the back-up algorithm.

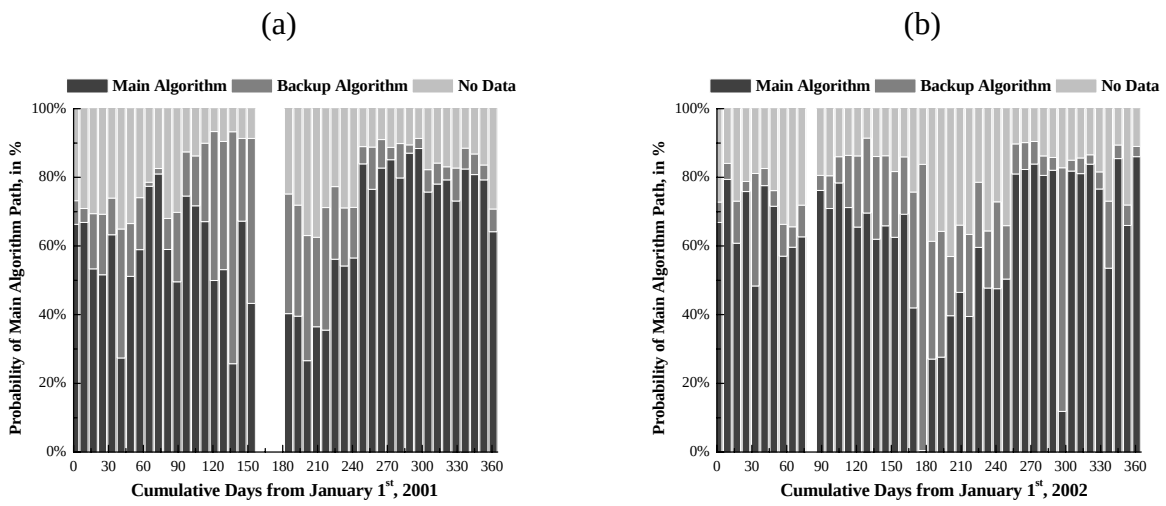

Fig. 5. Percentage of biome 1 pixels in the tile h10v05 processed by the main and the NDVI-based back-up algorithm.

(a)

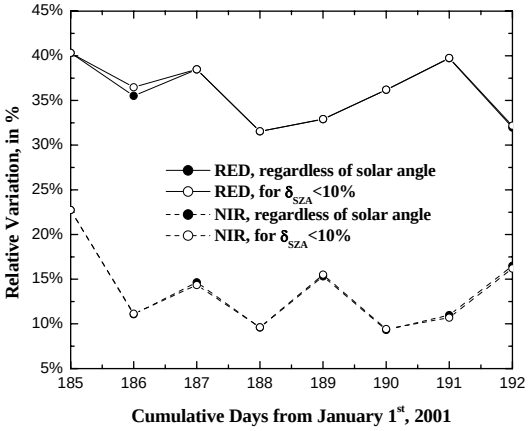

(b)

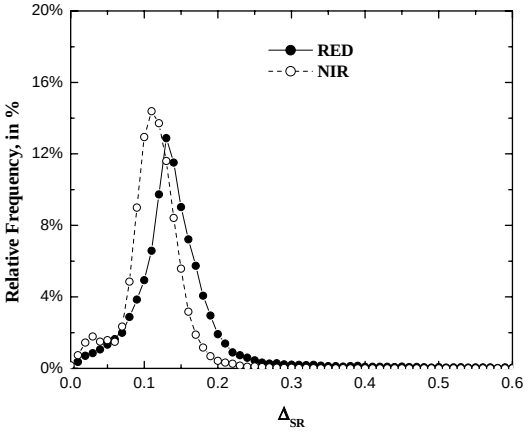

(c)

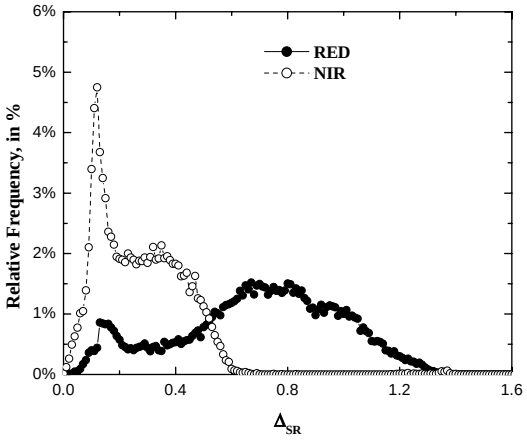

Fig. 6. Variations in MODIS surface reflectance data. (a) Daily variations in MODIS surface reflectances at red (RED) and near-infrared (NIR) spectral bands. Legends "RED, regardless of solar angle" and "NIR, regardless of solar angle" correspond to coefficients of variation (standard deviation/mean) calculated using all biome 1 (grasses and cereal crops) pixels in tile h10v05. Coefficients of variation calculated from pixels for which differences in the solar zenith angle did not exceed 10% are labeled as "Red, for Δ_{SZA}<10%" and "NIR, for Δ_{SZA}<10%". (b) Histogram of the coefficients of variation of MODIS surface reflectance at red and near-infrared bands derived for "Good Quality" data. (c) Same as (b) except that the coefficients of variation were derived from "Poor Quality" data. See section 4.1 for definitions of such data.

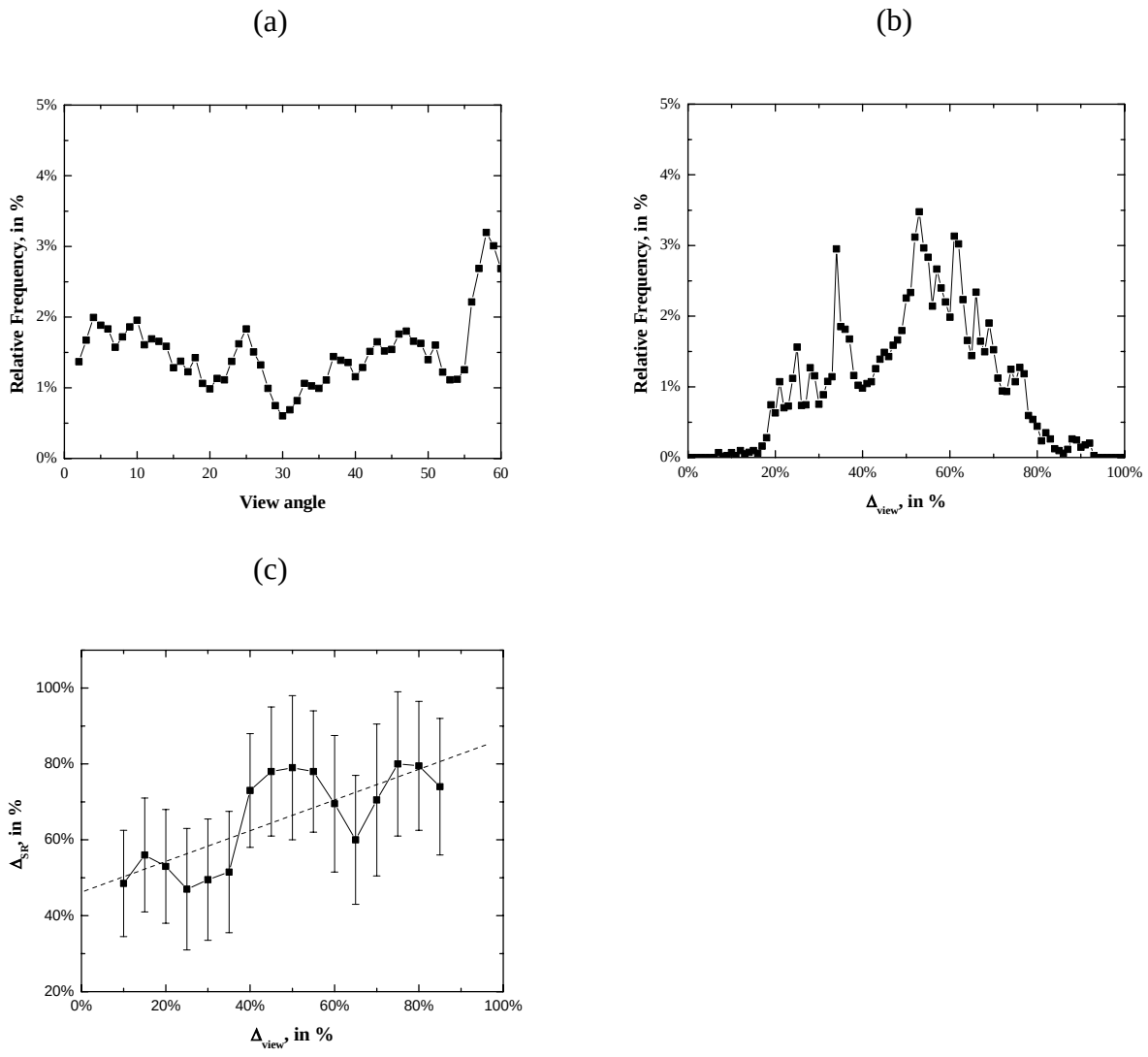

Fig. 7. Variations in MODIS surface reflectance data due to view angle changes. (a) Histogram of view angles for the set of "Poor Quality" pixels. (b) Histogram of δ_{view} (coefficient of variation of view angle) for the set of "Poor Quality" pixels. (c) Best possible prediction of variation, δ_{SR}, in surface reflectance at Red given variation, δ_{view}, in the view angle. The linear approximation of the regression curve is shown as straight line, $\delta_{\text{SR}} = 0.3\delta_{\text{view}} + 46\%$.

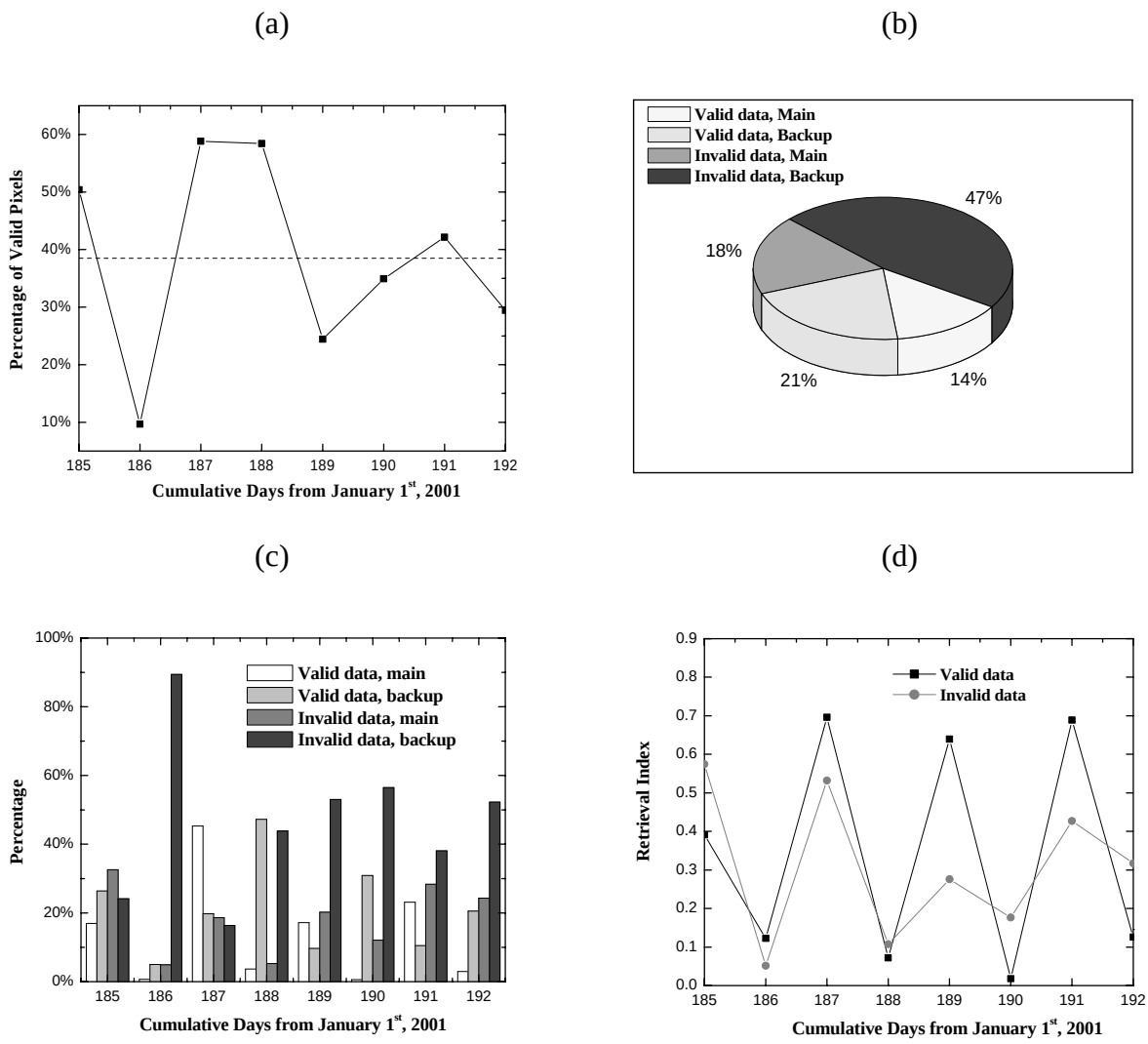

Fig. 8. Algorithm flow as function of input surface reflectance quality. (a) The ratio of valid pixels to total biome 1 (grasses and cereal crops) pixels, in percentage. The average ratio is shown here as a dashed line. (b) Distribution of valid and invalid pixels processed by the main and back-up algorithms. (c) Daily distribution of valid and invalid pixels processed by the main and back-up algorithms. (d) Daily variation in the retrieval index for valid and invalid pixels. The retrieval index is the fraction of processed pixels for which the main algorithm produces a retrieval. Average indices are shown in this plot as a dashed line.

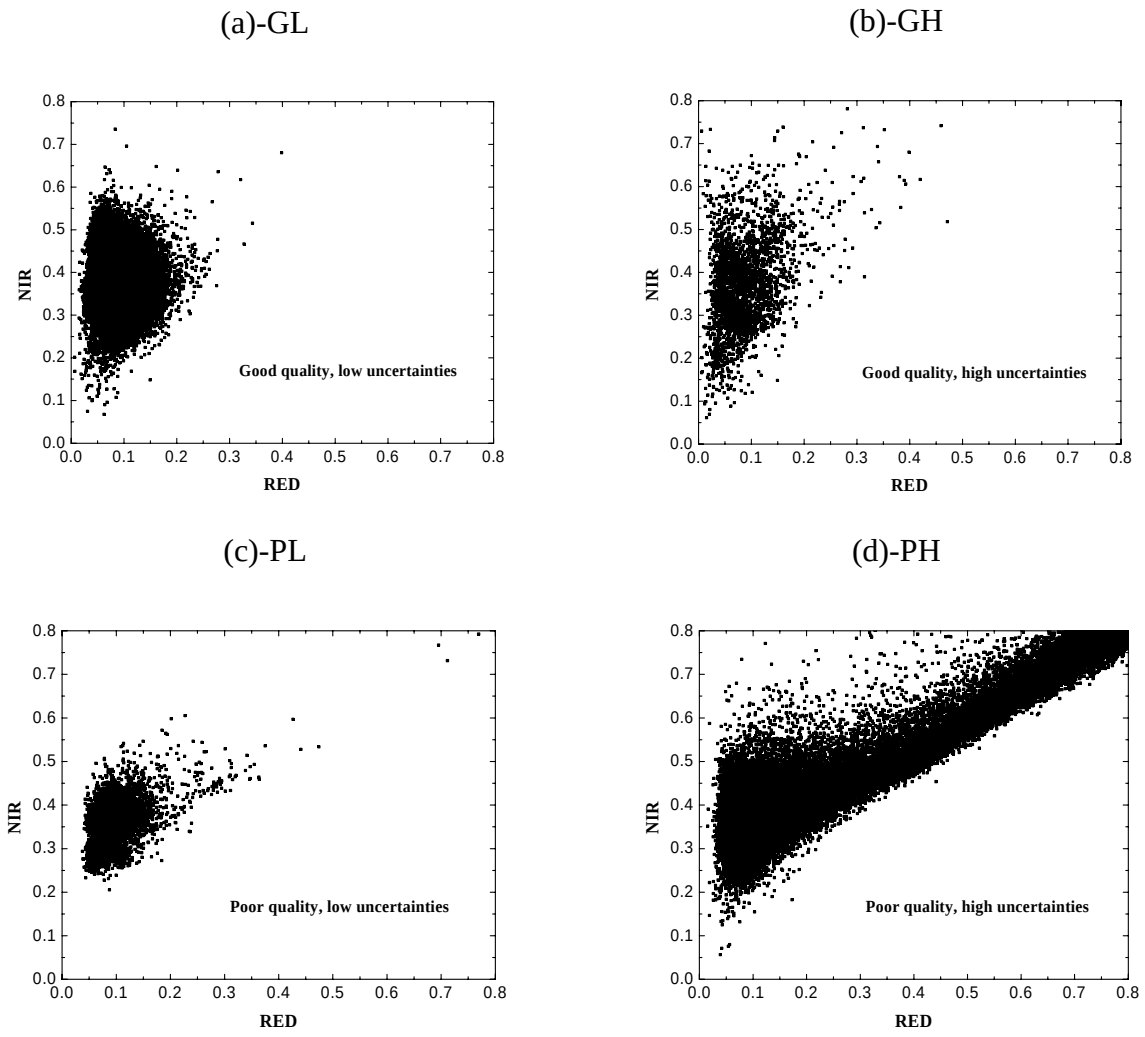

Fig. 9. Distribution in the red and near-infrared reflectance space of MODIS surface reflectance data from pixels with (a) good quality data and uncertainties less than 13% (GL) (b) good quality data and uncertainties greater than 13% (GH), (c) poor quality data and uncertainties less than 13% (PL) and (d) poor quality data and uncertainties greater than 13% (PH).

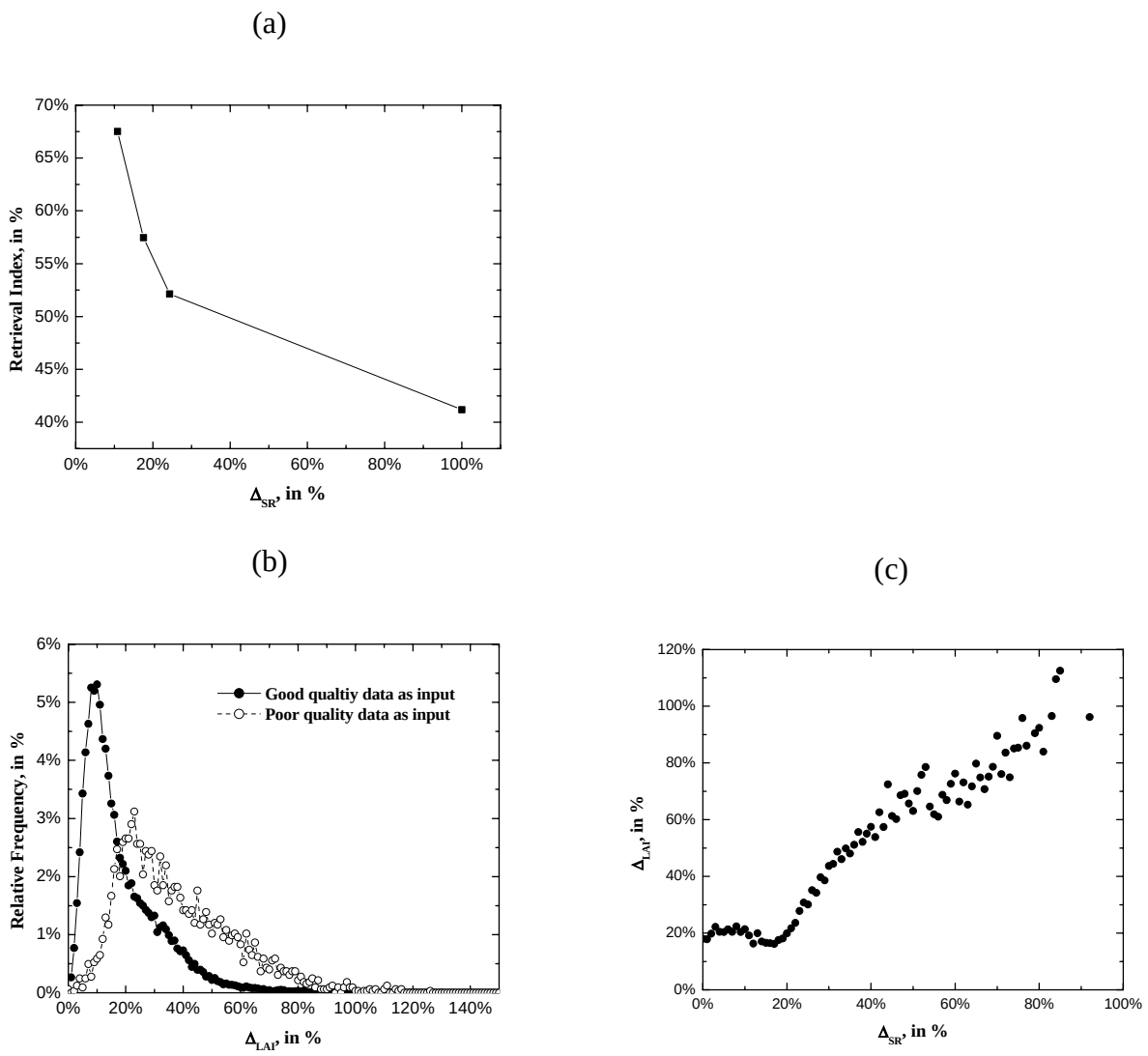

Fig 10. Impact on input reflectance data uncertainties on retrieval index and retrieval quality. (a) Retrieval index as a function of uncertainties in input surface reflectances. (b) Histograms of the coefficient of variation of LAI, δ_{LAI}, derived from good and poor quality pixels. (c) Uncertainties in LAI retrieval as a function of uncertainties in input surface reflectances.

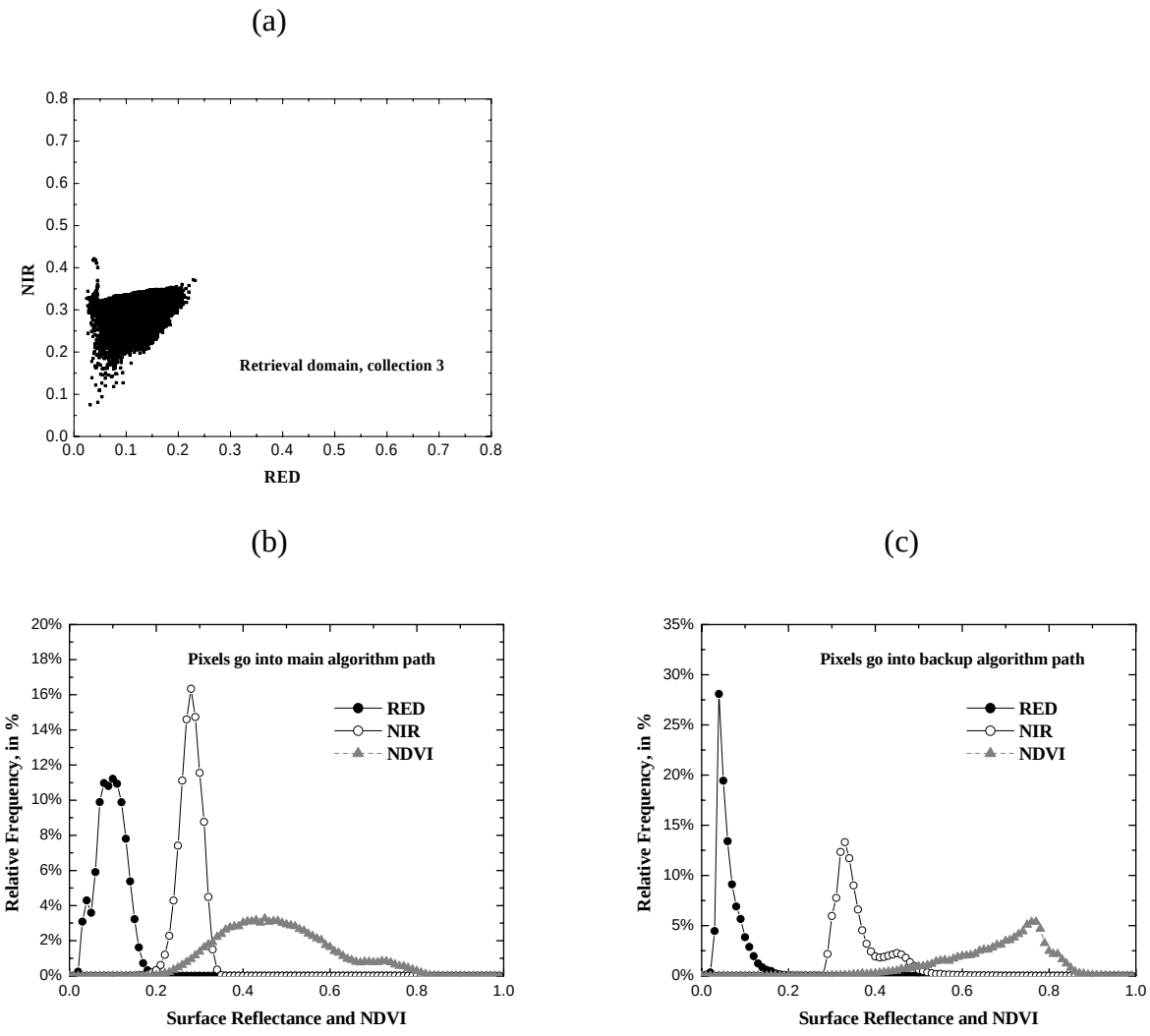

Fig. 11. Comparison of simulated and observed MODIS surface reflectances. (a) Distribution of biome 1 pixels in the red and near-infrared reflectance space as presently implemented in the Collection 3 MODIS LAI and FPAR algorithm. (b) Histogram of surface reflectance in the red, NIR bands and NDVI of pixels for which the main algorithm produces a LAI value. (c) Same as (b) except that for these pixels the main algorithm fails.

Table 1. Theoretical estimates made prior to launch of Terra MODIS of relative uncertainties in atmospherically corrected surface reflectances (Vermote, 2000).

Spectral Band	1 (Red)	2 (NIR)	3 (Blue)	4 (Green)
Center of Band, nm	670	865	443	555
Bandwidth, nm	20	40	20	20
Relative Error, %	10-33	3-6	50-80	5-12

Table 2. Spectral reflectance magnitudes of biome 1 (grasses and cereal crops) from MODIS, SeaWiFS and Landsat TM data.

	MODIS July, 2001	*SeaWiFS July, 1998*	*Landsat TM June 26, 1987*
Resolution	1 km	8 km	30 m
Averaging area	tile	global	Northwest USA
Mean Red reflectance	0.09	0.1	0.07
Mean NIR reflectance	0.35	0.24	0.30

Table 3. Comparison of observed and simulated surface reflectances.

	Collection 3 (C3)		Collection 4 (C4)		Good quality, low uncertainties (GL)		Good quality, high uncertainties (GH)		Poor quality, low uncertainties (PL)		Poor quality, high uncertainties (PH)	
	∩	∪	∩	∪	∩	∪	∩	∪	∩	∪	∩	∪
Collection 3 (C3)	2216	2216	2069	2335	755	3585	485	3157	247	2641	703	7555
Collection 4 (C4)			2278	2278	866	3626	577	3217	302	2738	798	7612
Good quality, low uncertainties (GL)					2214	2214	1216	2470	704	2274	1856	6490
Good quality, high uncertainties (GH)							1516	1516	529	1749	1186	6462
Poor quality, low uncertainties (PL)									762	762	754	6140
Poor quality, high uncertainties (PH)											6122	6122